



## Statistical downscaling of climate change impacts on ozone concentrations in California

Abdullah Mahmud,<sup>1</sup> Mary Tyree,<sup>2</sup> Dan Cayan,<sup>2</sup> Nehzat Motallebi,<sup>3</sup> and Michael J. Kleeman<sup>1</sup>

Received 24 October 2007; revised 18 August 2008; accepted 27 August 2008; published 7 November 2008.

[1] The statistical relationship between the daily 1-hour maximum ozone ( $O_3$ ) concentrations and the daily maximum upper air temperature was explored for California's two most heavily polluted air basins: the South Coast Air Basin (SoCAB) and the San Joaquin Valley Air Basin (SJVAB). A coarse-scale analysis of the temperature at an elevation of 850-mbar pressure (T850) for the period 1980–2004 was obtained from the National Center for Environmental Prediction (NCEP)/National Center for Atmospheric Research (NCAR) Reanalysis data set for grid points near Upland (SoCAB) and Parlier (SJVAB). Daily 1-hour maximum ozone concentrations were obtained from the California Air Resources Board (CARB) for these locations over the same time period. The ozone concentrations measured at any given value of the Reanalysis T850 were approximately normally distributed. The 25%, 50%, and 75% quartile ozone concentrations increased linearly with T850, reflecting the effect of temperature on emissions and chemical reaction rates. A 2D Lagrangian (trajectory) form of the UCD/CIT photochemical air quality model was used in a perturbation study to explain the variability of the ozone concentrations at each value of T850. Wind speed, wind direction, temperature, relative humidity, mixing height, initial concentrations for VOC concentrations, background ozone concentrations, time of year, and overall emissions were perturbed in a realistic fashion during this study. A total of 62 model simulations were performed, and the results were analyzed to show that long-term changes to emissions inventories were the largest sources of ozone variability at a fixed value of T850. Projections of future T850 values in California were obtained from the Geophysical Fluid Dynamics Laboratory (GFDL) model under the Intergovernmental Panel on Climate Change (IPCC) A2 and B1 emissions scenarios for the years 2001 to 2100. The future temperature trends combined with the historical statistical relationships suggest that an additional 22–30 days year<sup>-1</sup> in California would experience  $O_3 \geq 90$  ppb under the A2 global emissions scenario, and an additional 6–13 days year<sup>-1</sup> would experience  $O_3 \geq 90$  ppb under the B1 global emissions scenario by the year 2050 (assuming the  $NO_x$  and VOC emissions remained at 1990–2004 levels). These calculations help to quantify the climate “penalty” that must be overcome to improve air quality in California.

**Citation:** Mahmud, A., M. Tyree, D. Cayan, N. Motallebi, and M. J. Kleeman (2008), Statistical downscaling of climate change impacts on ozone concentrations in California, *J. Geophys. Res.*, 113, D21103, doi:10.1029/2007JD009534.

### 1. Introduction

[2] Peak 1-hour average ozone concentrations in California have declined from 375 ppb during the year 1985 to 175 ppb in the year 2004 [Cox *et al.*, 2006] because of the adoption of a long list of emissions controls. Health-based

ambient air quality standards for ozone concentrations are 90 ppb (California 1-hour standard) or 85 ppb (federal 8-hour standard revised to 75 ppb in 2008) indicating that further progress is needed to protect public health. As of 2007, 35 out of California's 58 counties are designated non-attainment areas for the federal 8-hour ozone standard, affecting the health of ~30 million residents.

[3] California has one of the largest economies in the world with correspondingly high emissions of air pollutants. The persistence of California's ozone problem is associated with warm sunny days with stagnant atmospheric conditions that trap emissions close to the surface where they have ample opportunity to undergo photochemical reactions. Climate change is expected to alter the long-term meteorological

<sup>1</sup>Department of Civil and Environmental Engineering, University of California, Davis, California, USA.

<sup>2</sup>Scripps Institute of Oceanography, University of California, San Diego, La Jolla, San Diego, California, USA.

<sup>3</sup>Research Division, California Air Resources Board, Sacramento, California, USA.

logical patterns in California, with potential negative consequences for air quality. Surface ozone is particularly sensitive to climate change because the chemical reactions that form ozone are temperature dependent, with higher levels of ozone produced during warmer time periods [Aw and Kleeman, 2003; Seinfeld and Pandis, 2006; Sillman and Samson, 1995]. In addition, biogenic emissions and anthropogenic evaporative emissions of volatile organic compounds (VOCs), which are precursors to ozone formation, will also increase with rising temperature [Constable et al., 1999; Fuentes et al., 2000; Rubin et al., 2006; Sanderson et al., 2003].

[4] Quantitative analysis of climate impacts on future ozone concentrations can be accomplished by dynamically downscaling Global Climate Model (GCM) results to regional scales using mesoscale meteorological models and regional air quality models [see for example, Dawson et al., 2007; Hogrefe et al., 2004; Steiner et al., 2006]. The dynamic approach incorporates a mechanistic description of atmospheric processes allowing it to extrapolate outside historical conditions. Unfortunately, the dynamic approach is also very computationally expensive in regions with severe topography such as California, and it may not yield accurate results if the description of the relevant atmospheric processes is incomplete.

[5] The statistical downscaling approach originally developed for hydrologic variables [Snyder et al., 2004] provides a promising alternative technique to evaluate climate effects on ozone concentrations. The statistical downscaling method relates coarse-scale meteorological variables that are available directly from GCM simulations to fine-scale outcomes. The statistical approach is computationally efficient and guaranteed to capture the behavior of the historical atmospheric conditions. The disadvantage of the statistical downscaling approach is that future conditions may not follow the historical pattern because of the changes in the emissions, and separate statistical relationships need to be identified for each air basin of interest. Dynamic and statistical downscaling techniques are complementary and both methods should be used to evaluate future ozone trends in California.

[6] The purpose of this paper is to develop a statistical downscaling approach for climate effects on surface ozone concentrations in two major air basins in California: the South Coast Air Basin (SoCAB) and the San Joaquin Valley Air basin (SJVAB). On the basis of an extensive review of all meteorological data, the upper air temperature at 850-mbar pressure (T850) ( $\sim 1.5$  km altitude) will be used as the independent variable for the analysis. The variability in the measured ozone concentration at a fixed value of T850 will be explored using a perturbation analysis conducted with a mechanistic photochemical trajectory model. The verified statistical downscaling techniques will be used to evaluate climate effects on future ozone formation potential for the years between 2001–2100 using the output from the Geophysical Fluid Dynamics Laboratory (GFDL) coupled Climate Model (CM2.1).

## 2. Data and Methods

[7] The daily maximum upper air temperatures at 850 mbar (T850) for the period 1980–2004 were obtained from the

National Center for Environmental Prediction (NCEP)/National Center for Atmospheric Research (NCAR) Reanalysis I [Bell et al., 2007] at two grid points near - (1) Upland in the South Coast Air Basin (SoCAB) and (2) Parlier in the San Joaquin Valley Air Basin (SJVAB). The NCEP/NCAR reanalysis assimilates historical measurements using the spectral statistical interpolation (SSI) scheme for the entire globe with a grid-cell size of  $2.5^\circ(\text{longitude}) \times 2.5^\circ(\text{latitude})$ . The resulting gridded data are saved at the beginning of each 6-hour interval (4 values saved each day). In the current project, the maximum of the 4 daily T850 values was used as the independent variable for correlation with ozone concentrations. Upper air temperature is considered to be among the most reliable data in the reanalysis data set (class A) because it is strongly constrained by direct observations [Kalnay et al., 1996].

[8] Projections of daily maximum T850 values for the period 2001–2100 were obtained from the Geophysical Fluid Dynamics Laboratory (GFDL) coupled climate model (CM2.1) [Delworth et al., 2006]. The daily model output was available with a grid cell size of  $2.5^\circ(\text{longitude}) \times 4^\circ(\text{latitude})$  in 6-hour intervals. Simulated climate from GFDL CM2.1 were used in the Fourth Assessment Report of the Intergovernmental Panel on Climate Change (IPCC). GFDL CM2.1 T850 simulated under the Special Reports on Emission Scenarios (SRES) categories A2 and B1 were also of particular importance for the first assessment of climate impacts in California [Cayan et al., 2008; Kalnay et al., 1996], and hence these T850 predictions were used in the current study.

[9] Daily 1-hour maximum ozone concentrations were provided by the California Air Resources Board (CARB) for two monitoring sites at: (1) Upland in the South Coast Air Basin (SoCAB) and (2) Parlier in the San Joaquin Valley Air Basin (SJVAB). The site at Upland (ARB ID: 36175, Lat:  $34^\circ 6' 14''$ , Lon:  $117^\circ 37' 35''$ , Elevation: 379 meters) is situated in a dense residential area east (downwind) of central Los Angeles. Ozone has been monitored continuously at Upland since 1 January 1973, and measurements for the period 1980–2004 were used in the current study. The site at Parlier (ARB ID: 10230, Lat:  $36^\circ 35' 50''$ , Lon:  $119^\circ 30' 15''$ , Elevation: 96 meters) is situated in an agricultural region southeast (downwind) of Fresno (the largest and urban center in the SJVAB). Although Parlier is located in a relatively remote area, it experiences major air pollution events with emission signatures from the greater Fresno area. Continuous ozone measurements are available since 1 January 1983 at Parlier, and data for the period 1990–2004 were used in the current study.

[10] Ozone concentrations at Upland and Parlier were measured with one of three possible instruments during the study period: a Dasibi 1003, and Dasibi 1008-AH, or an Advanced Pollution Instruments (API) 400. All monitors were regularly calibrated following a Standard Operating Procedure (SOP) so that the measurements remained accurate [SOP delivers  $\pm 3$ –10% bias] and consistent over a long period of time. A test was performed in the current study to verify that the apparent relationship between upper air temperature and ozone concentrations was stable across transition periods when monitors were changed. As expected, the use of different ozone analyzers did not

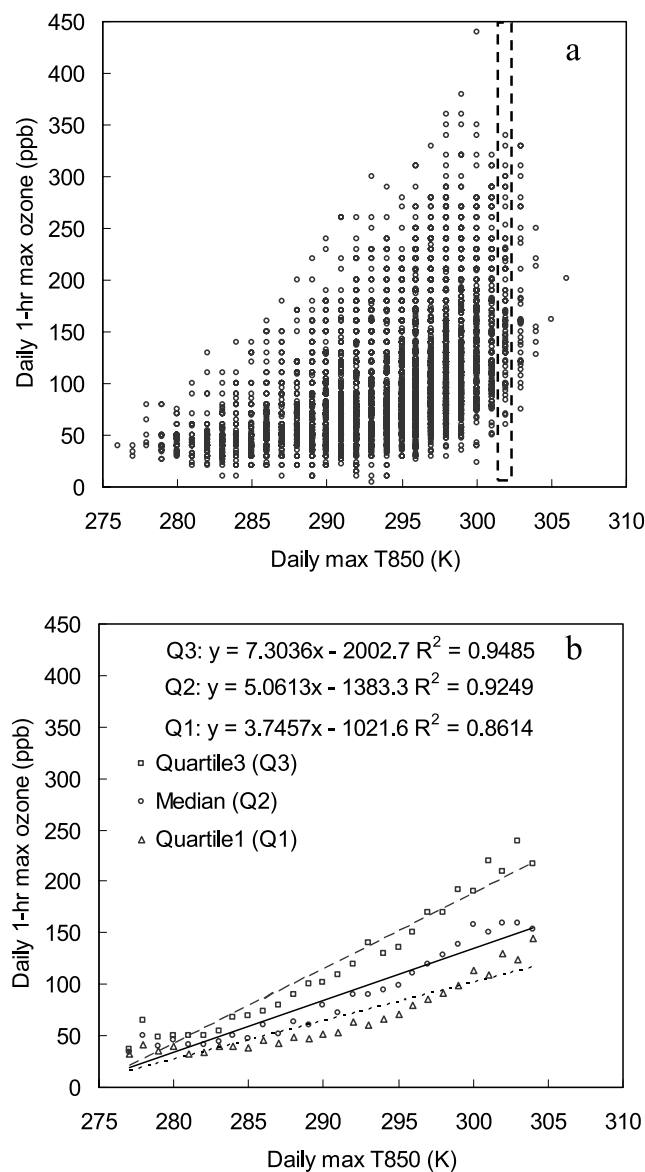


**Figure 1.** (a) Observed daily 1-hour max ozone versus the corresponding temperature at 850 mbar (T850) and (b) linear correlation between the ozone quartile boundaries and the corresponding daily max T850 at Upland, California, for the months May–October over the period 1980–2004.

significantly change the relationship between temperature and ozone.

[11] The variability in the relationship between ozone concentrations and T850 was explored in the current project using a 2D Lagrangian (trajectory) form of the University of California, Davis/California Institute of Technology (UCD/CIT) photochemical airshed model [Kleeman and Cass, 1998, 1999a, 1999b; Kleeman *et al.*, 1997, 1999]. The model tracks a  $5 \text{ km} \times 5 \text{ km}$  air parcel (5 vertical levels with a column height of 1100 meters) as it is advected across the domain of interest. Diagnostic meteorological fields and boundary (initial) concentrations are interpolated from measurements during the current study. The model tracks the emissions of pollutants from natural and anthropogenic sources, the vertical mixing of pollutants due to

turbulent diffusion, the reaction of pollutants due to photochemical processing, the condensation/evaporation of semi-volatile pollutants on primary particles, and deposition of pollutants to the surface of the earth. The Caltech Atmospheric Chemical Mechanism (CACM) [Griffin *et al.*, 2002a, 2002b] was used in the 2D Lagrangian model to predict the formation of ozone and other photochemical products. Previous studies have shown that CACM predictions for ozone and ozone precursors reproduce measured concentration trends at most sites in the SoCAB [Ying *et al.*, 2007].

### 3. Results

[12] Figure 1a shows the measured daily maximum 1-hour average ozone concentration as a function of the daily maximum T850 for the months May–October over the period 1980–2004 at Upland. Spring and fall months are included in the analysis even though they are outside the months that traditionally experience high ozone concentrations because climate change may increase the length of future “ozone seasons”. The scatter plot shows that the maximum observed ozone concentrations generally increased at higher temperatures, but there was significant variation at each T850 value, particularly between 281 K and 304 K. A linear correlation between ozone concentrations and the corresponding T850 is not obvious in Figure 1a because of the large variability in measured ozone concentrations at any given value of T850. Wind speed, wind direction, humidity, mixing depth, and  $\Delta T$  (elevated – surface) were also investigated as possible explanatory variables but they were not included in the final analysis because they did not significantly improve the regression statistics. Further study showed that the distribution of ozone concentrations at each T850 value was similar in shape but the median ozone concentration (second quartile; Q2) increases with T850. Likewise, the first (Q1) and third (Q3) quartile ozone concentrations also increase with T850. Figure 1b shows linear regressions between the quartiles (Q3, Q2-median and Q1) of the measured ozone concentrations and T850. The high  $R^2$  values ( $>0.80$ ) and the good agreement over a broad range of temperatures suggest that the correlation between quartile ozone concentrations and T850 holds true at all relevant temperatures in the South Coast Air Basin (SoCAB). This relationship reflects the positive influence that temperature has on ozone concentrations, even though other factors may also influence ozone concentrations. Figure 1b also reveals that the relationship between ozone and T850 flattens out below T850 values of 282 K. Ozone concentrations in this range are dominated by the background value of  $\sim 30$ – $40$  ppb that is advected into the South Coast Air Basin (SoCAB).

[13] Figure 2a shows the frequency distribution of maximum 1-hour average ozone concentrations measured at Upland when T850 was 302 K between May–October during the period 1980–2004. The distribution of ozone concentrations at this temperature was taken from the dashed rectangle shown in Figure 1a. Each ozone “bin” illustrated in Figure 2a shows the total number of days when maximum 1-hour average ozone concentrations reached the level indicated on the horizontal axis divided by the total number of days with T850 = 302 K. Figure 2 therefore



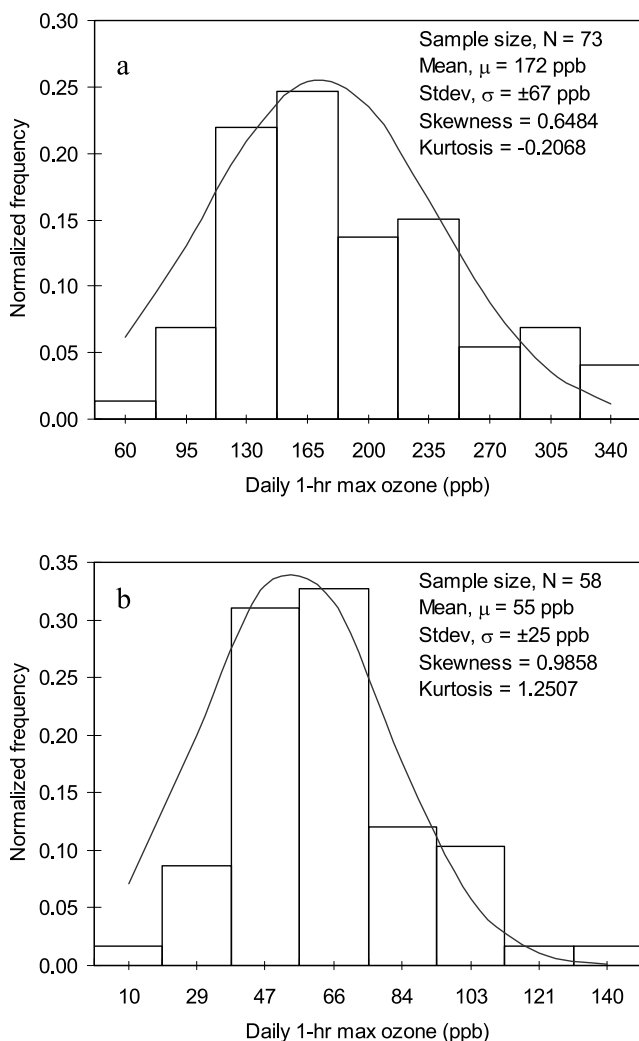


**Figure 2.** The frequency distributions of the observed daily 1-hour max ozone corresponding to T850 of (a) 302 and (b) 284 K at Upland, California, between May and October over the time period from 1980 to 2004.

shows the probability distribution of ozone concentrations at this location for this meteorological condition. The probability distribution is approximately normal with a mean ozone concentration of 172 ppb, a standard deviation of 67 ppb, and slight skewness (0.65) toward higher values of the ozone distribution. Similar probability distributions are associated with other values of T850. Figure 2b illustrates the probability distribution of ozone for T850 = 284 K. As shown in Figure 1b, the median concentration of each distribution is positively correlated with temperature. The variance of the probability distribution reflects the degree to which variables other than temperature influence ozone concentrations.

[14] One of the key objectives of this work was to identify the dominant sources of variability in the ozone frequency distribution that occurs at a given T850. The UCD/CIT air quality model that represents all major ozone formation processes was applied to study this question. The 2D Lagrangian form of the model was used in a Monte-Carlo simulation at Claremont, California, on 9 September 1993 in order to understand the dominant sources that

contribute to the variability of ozone concentrations at a given T850. Claremont was chosen as the receptor site because it is located in the eastern portion of the SoCAB where ozone concentrations are highest (similar to Upland) and numerous previous studies have been conducted at Claremont to validate the relevant meteorology databases and emissions inventories [Harley *et al.*, 1993; Kleeman and Cass, 1998; Ying *et al.*, 2007]. Three-day back trajectory routes for air parcel arriving at Claremont were calculated for each hour on 9 September 1993. The base case trajectory routes were then perturbed by adding stochastic bias to the wind-field [Bergin *et al.*, 1999; Kleeman *et al.*, 1999]. This method implicitly modifies dispersion coefficients, since dispersion is a function of wind speed. A total of 62 trajectory routes, including the base route were calculated for each hour of the day. Figure 3 shows the three-day back trajectory routes of air parcel arriving at Claremont at 3 pm on 9 September 1993, as an example.

[15] The Lagrangian form of the UCD/CIT air quality model was applied to each of the (5 km \* 5 km) air parcels trajectories ending at Claremont. Perturbations (summarized in Table 1) were introduced to the meteorological parameters, initial conditions (global background concentrations), and emissions to simulate variability that could occur in the real atmosphere. The magnitude of the temperature, mixing height and relative humidity perturbations was calculated using the measured distribution of historical values in the vicinity of Claremont. The magnitude of the emissions perturbations were chosen as an extreme case to estimate the maximum sensitivity associated with this variable [Kleeman and Cass, 1999b]. All perturbations were normally distributed with a mean value of zero. In addition to the emissions perturbations shown in Table 1, the base biogenic and evaporative emissions were scaled in response to changes in the perturbed temperature field. Biogenic emissions were adjusted using an exponential relationship between temperature and emissions rates developed by Guenther *et al.* [1993]. Evaporative emissions from mobile sources were adjusted using a linear relationship between temperature and emissions rates (evaporative emissions scaling factor =  $1 + (T - T_{ref}) * 1.34$  where  $T_{ref} = 20^{\circ}\text{C}$ ). This approximate equation was determined by running the Emission FACTor (EMFAC) model under different temperature scenarios and then taking the average response for the entire air basin (B. Hancock, California Air Resources Board, personal communication, 2007). Background ozone concentrations were taken to be random values normally distributed with a mean value of 45 ppb and a standard deviation of 5 ppb. The background (initial and boundary) concentrations for volatile organic compounds (VOC), oxides of nitrogen ( $\text{NO}_x$ ) and carbon monoxide (CO) were 18 ppb, 2 ppb and 200 ppb, respectively, at all model heights. The background value of methane ( $\text{CH}_4$ ) was set to zero as  $\text{CH}_4$  has no or little effect on regional-scale photochemical ozone production. To account for seasonal changes to the intensity of ultra violet (UV) radiation, the date was randomly selected between 1 May and 31 October.

[16] Figure 4 illustrates the frequency distribution and relevant statistical properties of the predicted ozone concentrations resulting from all of the Monte Carlo simulations summarized in Table 1. Figure 4a shows the distribution based on the emission inventory appropriate

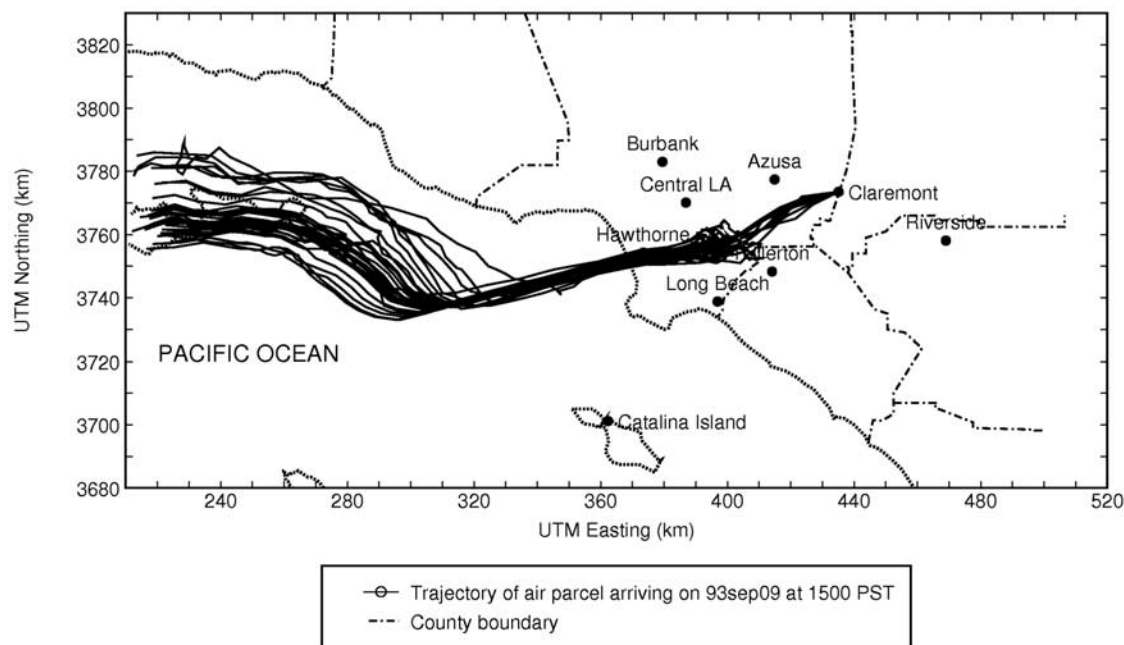


**Figure 3.** Three-day back trajectories for air parcel arriving at 12:00 pm on 9 September 1993 at Claremont, California. Each trajectory path reflects random variations in wind speed and direction.

for 1993 [Griffin *et al.*, 2002b; Ying *et al.*, 2007]. The modeled standard deviation (44 ppb) for this level of base emissions was less than that of the observed data (67 ppb) appropriate for  $T_{850} = 302\text{K}$ . The larger variance in the observed ozone concentrations may result from the long time period over which measurements were made (1980–2004). The emissions inventory in the South Coast Air Basin (SoCAB) has changed significantly over the last three decades, but the model predictions summarized in Figure 4a were based exclusively on an emissions inventory appropriate for 1993. In order to partially account for the variability introduced by long-term emissions trends, the stochastic modeling summarized in Figure 4a was repeated for the same scenarios at Claremont but using a base emission inventory appropriate for 1987 [Harley *et al.*, 1993; Kleeman and Cass, 1998]. VOC emissions were projected to be 32% higher in 1987 than in 1993, while emissions of NO<sub>x</sub> were projected to be 7% lower. These changes are less than or equal to the size of the random perturbations introduced during Monte Carlo simulations, but they are applied to all emissions records uniformly. In contrast, the Monte Carlo simulations perturbed individual emissions records by  $\pm 30\%$ , but the total emissions experienced by each air parcel from hundreds of different sources were close to the basecase values. Figure 4b illustrates that when base case emissions are used from 1987, the median predicted ozone concentrations and the variance of predicted ozone concentrations are both larger than the observed statistics between 1980–2004. Figure 4c shows the average of cases described in Figures 4a and 4b. These results clearly indicate that the absolute value of ozone formation potential was more sensitive to the perturbations summarized in Table 1 under the emissions conditions encountered in 1987 than those in 1993. The modeling exercises conducted in the current study clearly identify long-term emissions trends as the dominant source of

variability in the long-term ozone record at Upland, California.

[17] Figure 5 illustrates the measured reduction in quartile ozone concentrations in the SoCAB during summer months (May–October) between the 1990s and 1980s. The measured reduction in the median ozone concentration was 32%. Figure 5 also illustrates the reduction in predicted quartile ozone concentrations based on changes to the emissions inventory using the meteorological perturbations discussed above (Figure 4a vs. Figure 4b). The predicted reduction in median ozone concentrations due to changes in the emissions inventory was 37%, showing excellent agreement with measured values. This comparison once again emphasizes that long-term emissions trends are the dominant source of variability in the long-term ozone record at Upland, California. Further mechanistic analysis of ozone sensitivity to meteorological variables and background concentrations in California is provided by Aw and Kleeman [2003], Kleeman [2008], and Steiner *et al.* [2006].

[18] The effects of long-term emissions trends and seasonal variations on measured ozone concentrations were further investigated by separately analyzing different time segments of the measured ozone data record. The complete data record was segregated into three time periods: 1980–1989, 1990–1999 and 2000–2004, and into separate

**Table 1.** Variables That Were Perturbed During the Monte Carlo Simulations of Ozone Formation

Variable	Variation Amount
Temperature	$\pm 5^\circ\text{C}$
Mixing height	$\pm 20\%$
Relative humidity	$\pm 10\%$
Overall emissions	$\pm 30\%$
Initial conditions for VOCs	$\pm 30\%$
Initial condition for background ozone	Between $\pm 5$ ppb
Biogenic and evaporative emissions	Temperature-dependent scaling

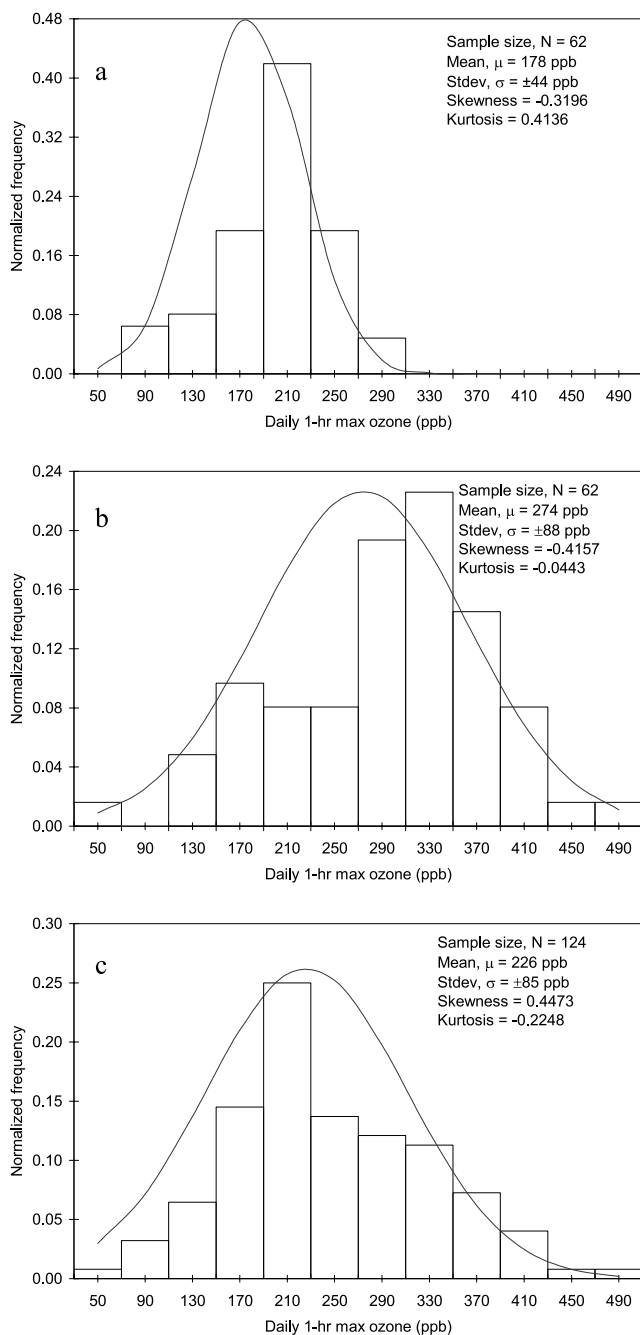


**Figure 4.** Predicted frequency distribution of the daily 1-hour maximum ozone concentration corresponding to a T850 of 302 K at Claremont, California. Different ozone values were generated by random perturbations in the input meteorological parameters, emissions, and initial conditions, as summarized in Table 1. Figure 4a corresponds to a base emission inventory appropriate for 1993, Figure 4b corresponds to base emission inventory appropriate for 1987, and Figure 4c represents the sum of Figures 4a and 4b.

months between May–October. The variability in the long-term ozone records is shown in Figure 6 as the correlation between the median ozone concentration and the corresponding T850 at Upland for the three different decades. The correlation slope (sensitivity) decreases from

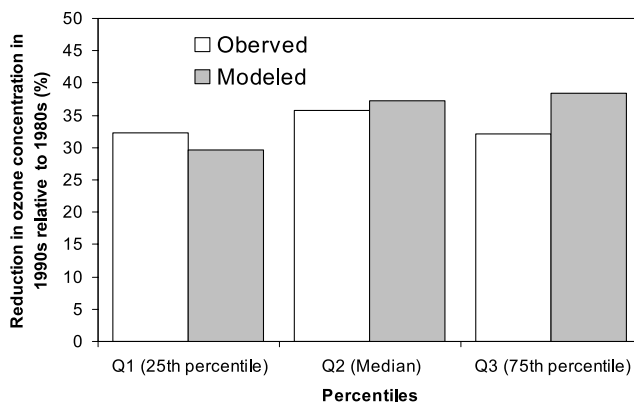


**Figure 5.** Comparison of observed and predicted reductions in ozone concentrations in 1990s relative to 1980s for the South Coast Air Basin (SoCAB) based on changes to the emissions inventory.

8.6 ppb  $K^{-1}$  for the period 1980–1989, to 6 ppb  $K^{-1}$  for the period 1990–1999, and 3.2 ppb  $K^{-1}$  for the period 2000–2004. The trend for 1990–1999 is in excellent agreement with the results from mechanistic modeling studies for 1993 and 1996 that predicted an ozone response to surface temperature of 2–9 ppb  $K^{-1}$  depending on location in the SoCAB [Kleeman, 2008]. The results in Figures 5 and 6 confirm the ability of the mechanistic model to capture climate effects on air quality and re-enforce the conclusion that long-term changes to the emissions inventory have decreased the sensitivity of absolute ozone concentrations to meteorological perturbations.

[19] The sensitivity of relative ozone concentrations to T850 changes as a function of the absolute ozone concentration (since the absolute sensitivity is linear over a range of ozone values). The relative sensitivity ( $\% K^{-1}$ ) at a fixed temperature can be calculated by dividing the constant value of the absolute sensitivity (ppb  $K^{-1}$ ) by the ozone concen-

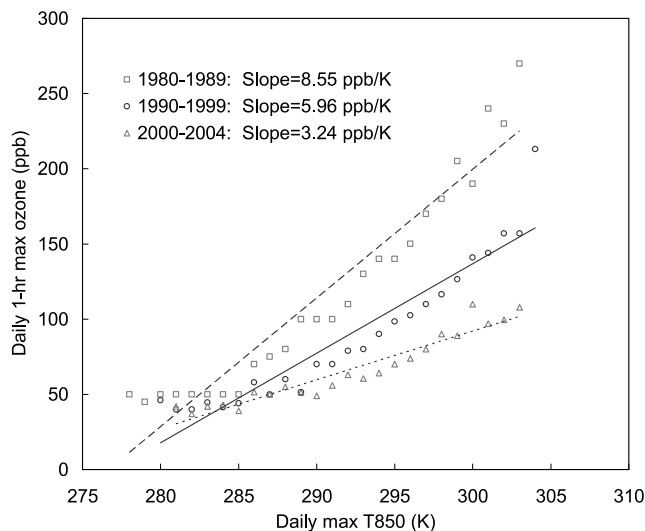


**Figure 6.** The linear correlation between the median of the observed daily 1-hour maximum ozone and the corresponding daily maximum T850 at Upland, California, as a function of decade.

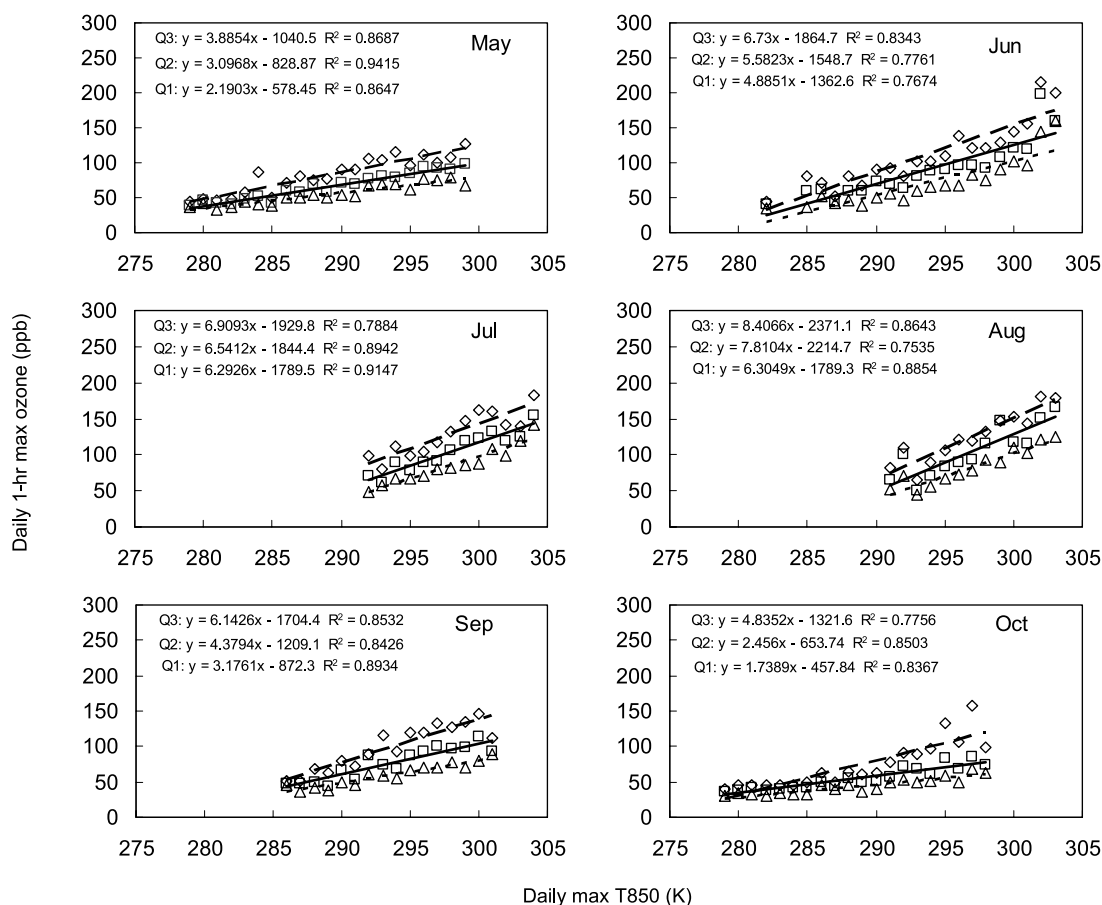


**Figure 7.** Seasonal correlation between 1-hour maximum ozone and 1-hour maximum T850 at Upland, California, for the years between 1990 and 2004. Diamonds correspond to quartile 3 (Q3), squares correspond to quartile 2 (median; Q2), and triangles correspond to quartile 1 (Q1).

tration (ppb) at the temperature of interest. Analysis of the data shown in Figure 6 reveals that the sensitivity of relative ozone formation at  $T850 \geq 300$  K is approximately constant at  $\sim 4.3\% \text{ K}^{-1}$  across each of the time periods that were studied. When  $T850 < 300$  K the calculated relative ozone sensitivity is influenced more strongly by the  $\sim 30\text{--}40$  ppb of background ozone that is transported into the air basin. Averaged across the entire range of temperatures illustrated in Figure 6, the relative sensitivity of ozone to temperature decreased from  $6\% \text{ K}^{-1}$  in 1980–89 to  $5.5\% \text{ K}^{-1}$  in 1990–99 and  $4.3\% \text{ K}^{-1}$  in 2000–04. Overall, the sensitivity of relative ozone formation appears to be constant at hotter temperatures and decreasing at cooler temperatures across the different time periods and emissions conditions studied.

[20] Ozone precursor emissions have decreased from 1980–1989 levels because of improved technology and stringent emission control measures, producing a decreasing trend in observed ozone concentrations [Cox *et al.*, 2006]. Future emissions changes may continue this downward trend, or they may rebound as population growth overtakes the effects of increased efficiency. In either case, emissions will be considered to be static at 1990–2004 levels for the remainder of the current study to allow for a direct analysis of climate change on ozone formation potential.

[21] Figure 7 shows the linear regression between ozone concentrations and Reanalysis T850 separately for different

summer months during the period 1990–2004 at Upland. The equations presented in the panels of Figure 7 represent the linear models based on the quartile ozone data. In each panel, the solid line represents the correlation based on the median ozone concentration and the upper and lower dashed lines indicate the correlation based on Q3 and Q1, respectively. The  $R^2$  values ( $>0.75$ ) indicate that the aggregated statistics of the ozone concentration distribution and T850 are well correlated. Importantly, different slopes are observed during different seasons. These reveal that ozone responds less strongly to temperature during the early spring (May–June) and late summer (September–October) months. Ozone concentrations respond most strongly to temperature during the middle of summer (July–August). The seasonal ozone response to T850 at Upland was also reanalyzed with a subset of the data points that have T850 between 291 K–301 K. Values of T850 in this range were measured in all months June–September within the historical data set, and so this analysis removes any potential bias associated with temperature extremes experienced in one month but not other months. The ozone response within the common temperature range at Upland was still stronger in July–August vs. June or September, suggesting that some other seasonal factor besides temperature is influencing the results. Monthly average mixing height measured between 1984–1991 at Oakland, California (at the coast upwind of



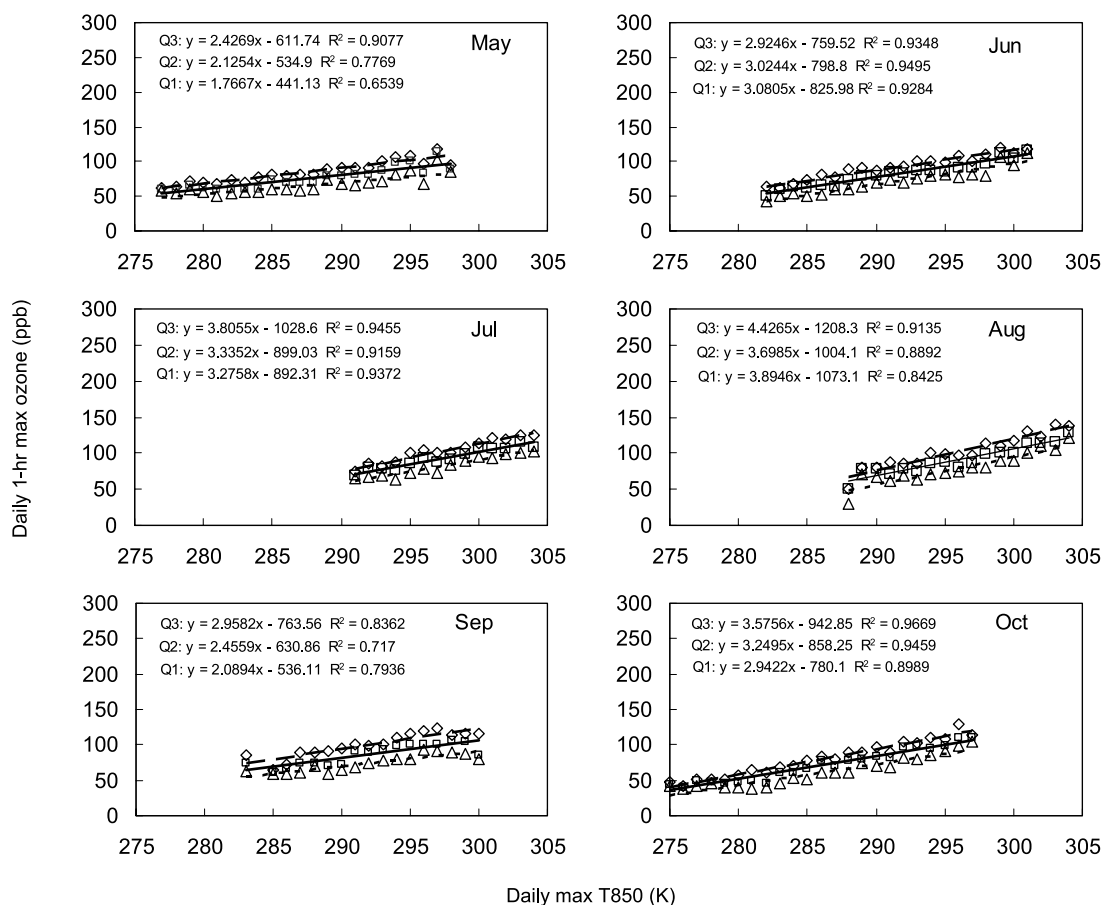


**Figure 8.** Seasonal correlation between 1-hour maximum ozone and 1-hour maximum T850 at Parlier, California, for the years between 1990 and 2004. Diamonds correspond to quartile 3 (Q3), squares correspond to quartile 2 (median; Q2), and triangles correspond to quartile 1 (Q1).

the SJVAB) varied from  $660 \pm 80$  m (June),  $550 \pm 75$  m (July),  $620 \pm 74$  m (August), and  $660 \pm 150$  m (September). Mixing depth can influence ozone production [Kleeman, 2008], but the inclusion of the best-available mixing depth information in the current study did not add skill to the statistical model. Another possible seasonal factor is trends in biogenic emissions as vegetation follows a seasonal growth cycle [see for example Geron *et al.*, 2000].

[22] Figure 8 shows the linear regression of quartile ozone concentrations from Reanalysis T850 at Parlier in the SJVAB for each month between May–October. Ozone trends in the SJVAB are qualitatively similar to those in the SoCAB, but the magnitude of the change induced by temperature is different because the underlying emissions inventories for the two air basins are not the same. Increased temperature still enhances ozone concentrations in the SJVAB, but the magnitude of the change is smaller than that observed in the SoCAB. As exhibited by the Upland analyses, July and August had the largest values of the regression slopes between ozone and T850 compared to other months.

[23] Future trends in upper air temperature are simulated by Global Climate Models (GCMs) in response to global change. There are several climate models currently available in the scientific community including the National Center for Atmospheric Research Parallel Climate Model version 1

(NCAR-PCM1), the NCAR-Community Climate System Model version 3 (NCAR-CCSM3), the Geophysical Fluid Dynamics Coupled Model version 2.1 (GFDL CM2.1), the Centre National de Recherches Meteorologiques Climate Model version 3 (CNRM-CM3) (French climate model), the Max Planck Institute for Meteorology ECHAM version 5 (MPI-ECHAM5) (German climate model), and the Model for Interdisciplinary Research on Climate version 3.2 (MIROC3.2) (medium resolution) (Japanese climate model). In the current study, the GFDL CM2.1 model was used to provide simulated T850 over a global domain, including California, for the years 2001–2100 based on several IPCC greenhouse gas emissions scenarios. Table 2 summarizes the temperature (T850) increase in California over the period 2070–2099 relative to 1961–1990 predicted by all of the GCMs described above. Decadal average results for all models are similar with a temperature increase of 4–5°C (A2 highest-emission scenario) or 3–4°C (B1 lowest-emissions scenario) during the summer ozone season in both the SJVAB and the SoCAB. The daily GFDL CM2.1 values of T850 simulated at coarse scale from model locations over the SoCAB and the SJVAB under the A2 and the B1 scenarios were used to estimate the potential for ozone formation in California. Ozone concentrations at Upland and Parlier were calculated based on the projected values of T850 for each day and the monthly statistical relationships



**Table 2.** Temperature (T850) Increase (°C) in 2070–2099 Relative to 1961–1990 Projected for the SoCAB and SJAB by Various Climate Models Under the IPCC A2 and B1 Emissions Scenario

Model	SoCAB				SJVAB			
	Jan–Mar		Jul–Sep		Jan–Mar		Jul–Sep	
	A2	B1	A2	B1	A2	B1	A2	B1
GFDL CM2.1	4	2	5	3	3	2	5	3
CNRM CM3	3	2	4	2	3	2	4	2
MIROC3.2 (med)	4	3	7	4	4	3	7	4
MPI ECHAM5	3	3	4	3	4	3	4	3
NCAR CCSM3	3	2	5	2	3	2	4	3
NCAR PCMI	2	2	2	1	2	2	3	2

between ozone and T850 illustrated in Figures 7 and 8 for the period 1990–2004. The median (Q2) ozone–T850 relationship in Figures 7 and 8 were used to obtain a baseline estimate, while Q1 and Q3 were used to obtain upper and lower bounds. In addition to the summer months (May–Oct), the correlations found in May and October were applied to each month of the periods February–April, and November–January, respectively. After calculating the daily 1-hour max quartile (Q1, Q2 and Q3) ozone concentrations with the projected temperature values for each year, the number of days with 90 ppb or more ozone was calculated for each month and an aggregate yearly result

was derived under the assumption that NO<sub>x</sub> and VOC emissions remained at 1990–2004 levels. The constant emissions reference of ozone precursors point was chosen to separately identify the projected effect of climate change on ozone concentrations.

[24] Figures 9 and 10 show the number of days in each year that would be likely to exceed the 90 ppb threshold of the daily maximum 1-hour average ozone concentrations at Upland and Parlier respectively, if emissions remained at the 1990–2004 level. The circle represents the number of days based on the median ozone estimate, and the top and bottom bars represent the number of days based on the Q3 and Q1 correlations, respectively. As can be seen in these figures, the upper and lower bars represent the breadth of the distribution of the number of days likely to exceed the daily ozone threshold of 90 ppb for each year because of increasing temperature effects. Data are presented for years between 2001–2100. In both the SoCAB and the SJVAB, future values of T850 are projected to increase under both the IPCC A2 and B1 emissions scenarios, leading to more days each year when ozone concentrations would exceed 90 ppb (under the assumption that NO<sub>x</sub> and VOC emissions remain at 1990–2004 level). The rate of increase is higher (0.5–0.7 days yr<sup>-1</sup>) for the A2 emissions scenario than the B1 emissions scenario (0.2–0.3 days yr<sup>-1</sup>) because greater temperature increases are predicted under the A2 emissions scenario.

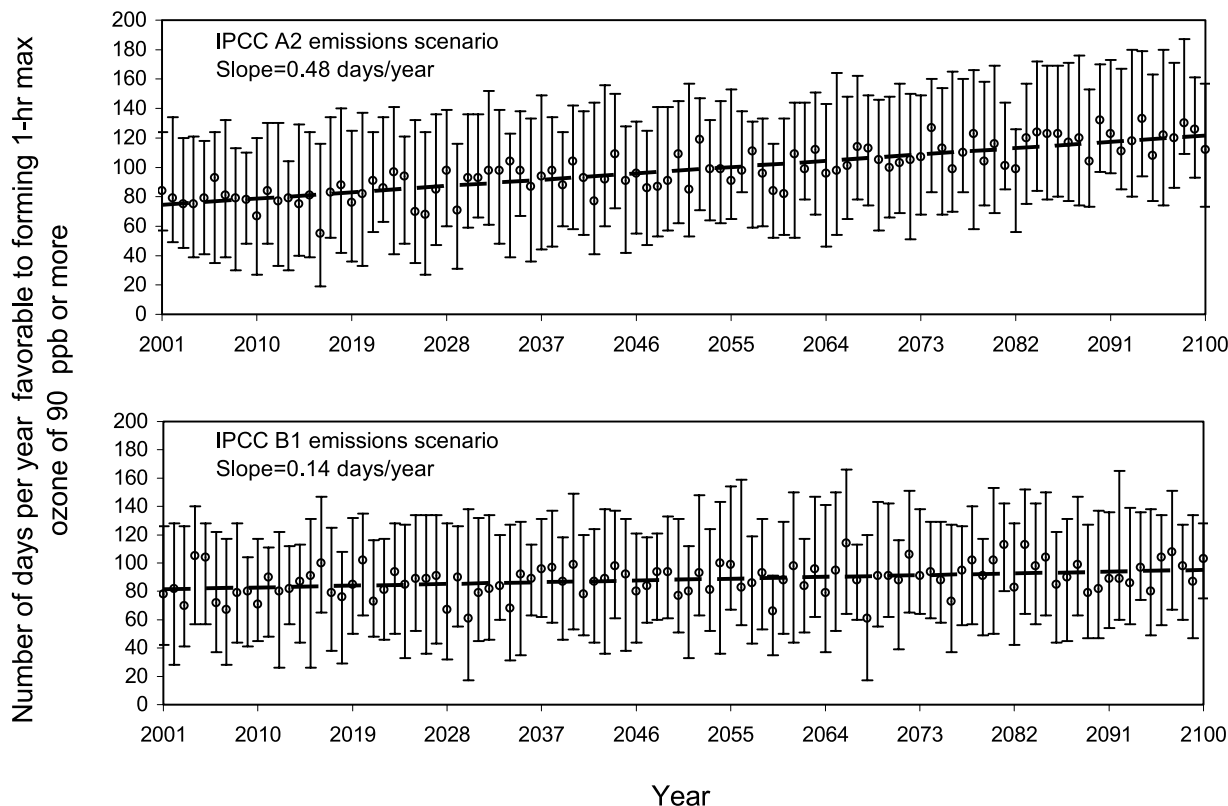


**Figure 9.** The number of days per year conducive to forming 1-hour maximum ozone of 90 ppb or more at Upland, California, under the Intergovernmental Panel of Climate Change (IPCC) emissions scenarios: (top) A2 and (bottom) B1. Note that the underlying assumption for this prediction is that the NO<sub>x</sub> and VOC emissions in California remain at the 1990–2004 level. Uncertainty bars represent the Q1 and Q3 estimates of the predicted number of days.

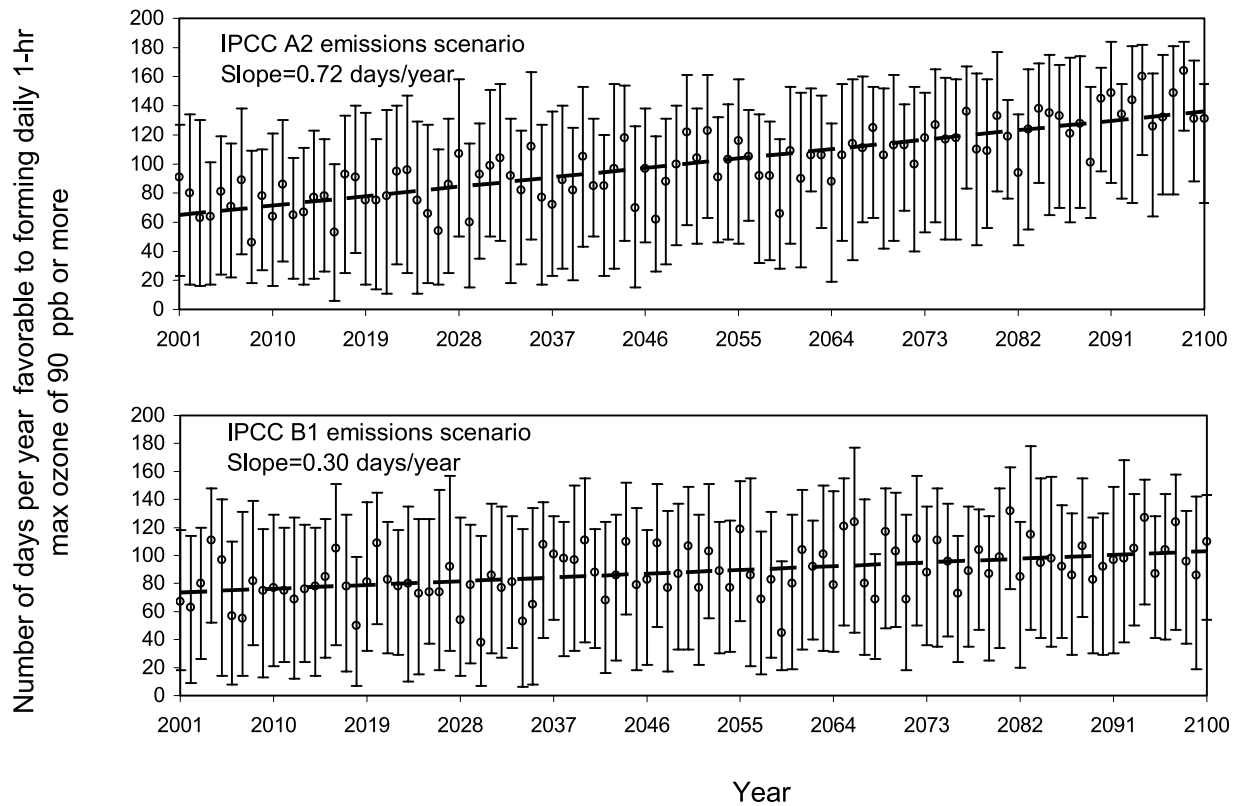


**Figure 10.** The number of days per year conducive to forming 1-hour maximum ozone of 90 ppb or more at Parlier, California, under the Intergovernmental Panel of Climate Change (IPCC) emissions scenarios: (top) A2 and (bottom) B1. Note that the underlying assumption for this prediction is that the  $\text{NO}_x$  and VOC emissions in California remain at the 1990–2004 level. Uncertainty bars represent the Q1 and Q3 estimates of the predicted number of days.

[25] The rate of increase for the number of days exceeding the 90 ppb ozone threshold at Parlier (SJVAB) is greater than at Upland (SoCAB) despite the fact that historical ozone concentrations are less sensitive to temperature at

Parlier during all months but October (compare Figure 7 to Figure 8). These apparently contradictory trends can be explained by examining the total number of days exceeding 90 ppb of ozone during each month of the years 2046–2055

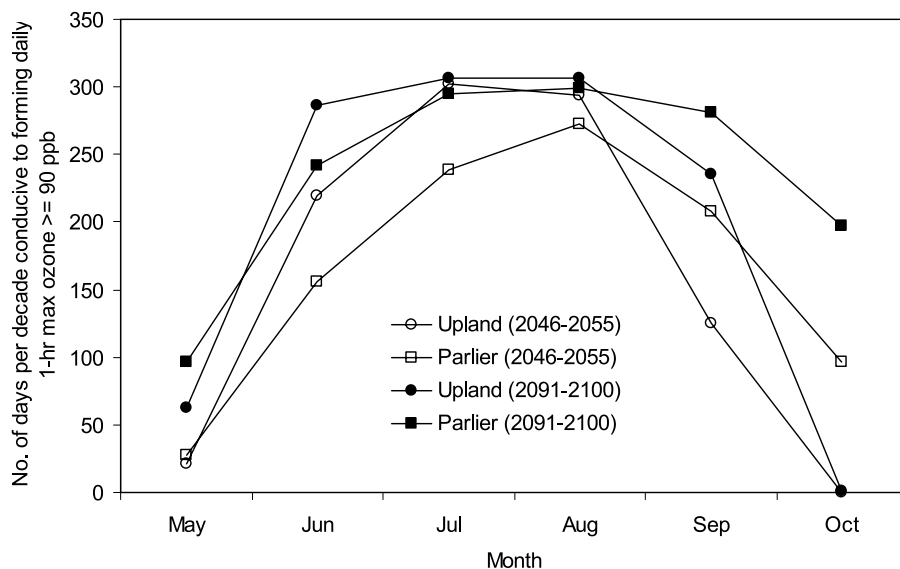


**Figure 11.** Number of days per decade conducive to the formation of daily 1-hour max ozone  $\geq 90$  ppb for 2046–2055 and 2091–2100 at Upland (SoCAB) and Parlier (SJVAB). Note that the underlying assumption for this prediction is that the  $\text{NO}_x$  and VOC emissions in California remain at the 1990–2004 level.

**Table 3.** Summary of Predicted Decadal Median Daily 1-Hr Maximum Ozone Concentrations Under IPCC A2 and B1 Global Emissions Scenarios at Upland (SoCAB) and Parlier (SJVAB)<sup>a</sup>

Decade	Median Ozone Concentration (ppb)			
	Upland (SoCAB)		Parlier (SJVAB)	
	A2	B1	A2	B1
2001–2010	84	84	86	87
2011–2020	84	87	87	87
2021–2030	86	86	88	86
2031–2040	92	87	90	89
2041–2050	90	87	90	89
2051–2060	92	87	92	88
2061–2070	97	89	93	91
2071–2080	100	91	96	90
2081–2090	105	92	97	91
2091–2100	111	91	101	92

<sup>a</sup>Note that the underlying assumption for this prediction is that the NO<sub>x</sub> and VOC emissions in California remain at the 1990–2004 level.

and 2091–2100 assuming emissions remained at 1990–2004 levels. Figure 11 illustrates that the months of July and August become “saturated” after ~2050 with continued increases occurring mainly in May–June and September–October. The annual growth at Parlier (SJVAB) is greater than Upland (SoCAB) primarily because of increases during the month of October. These trends reflect the greater lengthening of the “ozone season” in the SJVAB compared to the SoCAB assuming emissions remained constant at 1990–2004 levels.

[26] Table 3 illustrates the predicted seasonal (May–October) median daily 1-hour ozone concentration for each decade over the period 2001–2100 at Upland (SoCAB) and Parlier (SJVAB) under the IPCC A2 and B1 emissions scenarios. Generally, the predicted median ozone increases in both the SoCAB and SJVAB over time. The seasonal median daily 1-hour ozone concentration would exceed 90 ppb as early as in 2031–2040 under the warming induced by the A2 global emissions scenario assuming NO<sub>x</sub> and VOC emissions in California remain at the 1990–2004 level. Global Climate Models are not expected to accurately represent the weather during any given year but they should capture the meteorology over a period of decades. The GFDL CM2.1 model results were obtained for the period 1990–2000 and the T850 values were used to predict ozone concentrations based on the correlations derived in the current study. The average value of the 1-hour maximum daily ozone concentration was 84 ppb (predicted) vs. 97 ppb (measured) in the SoCAB and 83 ppb (predicted) vs. 85 ppb (measured) in the SJVAB for this period indicating that the statistical downscaling method developed in this study can effectively be used to project ozone concentrations in the future for a given air basin.

#### 4. Conclusion

[27] The daily maximum upper air temperature at an altitude of 850-mbar pressure (T850) taken from coarse-scale global model locations nearest to California’s two most polluted air basins can be used to model daily 1-hour maximum surface ozone concentrations in those air basins. Other explanatory variables including wind speed, wind direction, humidity, and mixing depth did not add skill to the

statistical model. There is not a one-to-one correlation between ozone and T850 extracted from the global Reanalysis data set, but the value of T850 can be used to predict the statistical properties of the possible range of ozone concentrations. These ozone concentration distributions are approximately normal and their 25%, 50% and 75% quartile concentrations are linearly correlated with temperature. By constructing separate linear regression models for each month of the year, the effects of seasonal changes on the ozone – T850 relationship can be represented. The response of ozone to T850 is strongest in July and August and weaker in spring, early summer and fall. The sensitivity of absolute ozone concentrations to T850 has decreased over the past several decades because of changes in anthropogenic emissions. Future anthropogenic emissions trends in California will depend on the balance between population growth vs. energy conservation and the further development of efficient technologies.

[28] The statistical relationship between coarse-scale T850 and fine-scale ozone concentrations provides an efficient technique to downscale global model circulation structure to local air basin ozone concentrations. The effect of climate on future ozone concentrations can be evaluated using average emissions levels between 1990–2004 as a constant reference point. Projections of future temperature made by the GFDL CM2.1 global climate model combined with the historical ozone trends suggest that, by the year 2050, the number of days with conditions likely to encourage ozone concentrations greater than 90 ppb would increase by 22–30 days yr<sup>-1</sup> under the IPCC SRES A2 emissions scenario and 6–13 days yr<sup>-1</sup> under the B1 emissions scenario. Warmer future temperatures will require the implementation of additional emissions controls in California to offset this climate “penalty”.

[29] **Acknowledgments.** This research was supported by the California Air Resources Board Project 04-349. D.R.C. and M.T. were funded by the California Energy Commission through the California Climate Change Center and by the NOAA RISA program through the California Applications Program. We thank Martha Coakley and Josh Shiffirin for data processing and analyses.

#### References

- Aw, J., and M. J. Kleeman (2003), Evaluating the first-order effect of intraannual temperature variability on urban air pollution, *J. Geophys. Res.*, 108(D12), 4365, doi:10.1029/2002JD002688.
- Bell, M. L., et al. (2007), Climate change, ambient ozone, and health in 50 US cities, *Clim. Change*, 82, 61–76.
- Bergin, M. S., et al. (1999), Formal uncertainty analysis of a Lagrangian photochemical air pollution model, *Environ. Sci. Technol.*, 33, 1116–1126.
- Cayan, D. R., et al. (2008), Climate change scenarios for the California region, *Clim. Change (Special Issue on Climate Change Scenarios)*, 87, S21–S42.
- Constable, J. V. H., et al. (1999), Modelling changes in VOC emission in response to climate change in the continental United States, *Global Change Biol.*, 5, 791–806.
- Cox, P., et al. (2006), *The California Almanac of Emissions and Air Quality*, Plann. and Tech. Support Div. Calif. Air Resour. Board, Sacramento, CA.
- Dawson, J. P., et al. (2007), Sensitivity of ozone to summertime climate in the eastern USA: A modeling case study, *Atmos. Environ.*, 41, 1494–1511.
- Delworth, T. L., et al. (2006), GFDL’s CM2 global coupled climate models. part I: Formulation and simulation characteristics, *J. Clim.*, 19, 643–674.
- Fuentes, J. D., et al. (2000), Biogenic hydrocarbons in the atmospheric boundary layer: A review, *Bull. Am. Meteorol. Soc.*, 81, 1537–1575.

- Geron, C., et al. (2000), Temporal variability in basal isoprene emission factor, *Tree Physiol.*, *20*, 799–805.
- Griffin, R. J., et al. (2002a), Secondary organic aerosol—3. Urban/regional scale model of size- and composition-resolved aerosols, *J. Geophys. Res.*, *107*(D17), 4334, doi:10.1029/2006JD000544.
- Griffin, R. J., et al. (2002b), Secondary organic aerosol—1. Atmospheric chemical mechanism for production of molecular constituents, *J. Geophys. Res.*, *107*(D17), 4332, doi:10.1029/2001JD000541.
- Guenther, A. B., et al. (1993), Isoprene and monoterpene emission rate variability—Model evaluations and sensitivity analyses, *J. Geophys. Res.*, *98*, 12,609–12,617.
- Harley, R. A., et al. (1993), Photochemical modeling of the Southern California air-quality study, *Environ. Sci. Technol.*, *27*, 378–388.
- Hogrefe, C., et al. (2004), Simulating changes in regional air pollution over the eastern United States due to changes in global and regional climate and emissions, *J. Geophys. Res.*, *109*, D22301, doi:10.1029/2004JD004690.
- Kalnay, E., et al. (1996), The NCEP/NCAR 40-year reanalysis project, *Bull. Am. Meteorol. Soc.*, *77*, 437–471.
- Kleeman, M. J. (2008), A preliminary assessment of the sensitivity of air quality in California to global change, *Clim. Change*, *87*, suppl. 1, 273–292.
- Kleeman, M. J., and G. R. Cass (1998), Source contributions to the size and composition distribution of urban particulate air pollution, *Atmos. Environ.*, *32*, 2803–2816.
- Kleeman, M. J., and G. R. Cass (1999a), Effect of emission control strategies on the size and composition distribution of urban particulate air pollution, *Environ. Sci. Technol.*, *33*, 177–189.
- Kleeman, M. J., and G. R. Cass (1999b), Identifying the effect of individual emissions sources on particulate air quality within a photochemical aerosol processes trajectory model, *Atmos. Environ.*, *33*, 4597–4613.
- Kleeman, M. J., G. R. Cass, and A. Eldering (1997), Modeling the airborne particle complex as a source-oriented external mixture, *J. Geophys. Res.*, *102*(D17), 21,355–21,372.
- Kleeman, M. J., et al. (1999), Source contributions to the size and composition distribution of atmospheric particles: Southern California in September 1996, *Environ. Sci. Technol.*, *33*, 4331–4341.
- Rubin, J. I., et al. (2006), Temperature dependence of volatile organic compound evaporative emissions from motor vehicles, *J. Geophys. Res.*, *111*, D03305, doi:10.1029/2005JD006458.
- Sanderson, M. G., et al. (2003), Effect of climate change on isoprene emissions and surface ozone levels, *Geophys. Res. Lett.*, *30*(18), 1936, doi:10.1029/2003GL017642.
- Seinfeld, J. H., and S. N. Pandis (2006), *Atmospheric Chemistry and Physics: From Air Pollution to Climate Change*, Wiley, New York.
- Sillman, S., and F. J. Samson (1995), Impact of temperature on oxidant photochemistry in urban, polluted rural and remote environments, *J. Geophys. Res.*, *100*(D6), 11,497–11,508.
- Snyder, M. A., et al. (2004), Modeled regional climate change in the hydrologic regions of California: A CO<sub>2</sub> sensitivity study, *J. Am. Water Resour. Assoc.*, *40*, 591–601.
- Steiner, A. L., et al. (2006), Influence of future climate and emissions on regional air quality in California, *J. Geophys. Res.*, *111*, D18303, doi:10.1029/2005JD006935.
- Ying, Q., et al. (2007), Verification of a source-oriented externally mixed air quality model during a severe photochemical smog episode, *Atmos. Environ.*, *41*, 1521–1538.

---

D. Cayan and M. Tyree, Scripps Institute of Oceanography, University of California, San Diego, La Jolla, San Diego, CA 92093, USA.

M. J. Kleeman and A. Mahmud, Department of Civil and Environmental Engineering, University of California, Davis, 1 Shields Avenue, Davis, CA 95616, USA. (mjkleeman@ucdavis.edu)

N. Motallebi, Research Division, California Air Resources Board, Sacramento, CA 95812, USA.